



Υ production in Z Decays

M. Acciarri, O. Adriani, M. Aguilar-Benitez, S. Ahlen, J. Alcaraz, G. Alemanni, J. Allaby, A. Aloisio, G. Alverson, M G. Alviggi, et al.

► To cite this version:

M. Acciarri, O. Adriani, M. Aguilar-Benitez, S. Ahlen, J. Alcaraz, et al.. Υ production in Z Decays. Physics Letters B, 1997, 413, pp.167-175. in2p3-00000220

HAL Id: in2p3-00000220

<https://hal.in2p3.fr/in2p3-00000220>

Submitted on 6 Nov 1998

HAL is a multi-disciplinary open access archive for the deposit and dissemination of scientific research documents, whether they are published or not. The documents may come from teaching and research institutions in France or abroad, or from public or private research centers.

L'archive ouverte pluridisciplinaire **HAL**, est destinée au dépôt et à la diffusion de documents scientifiques de niveau recherche, publiés ou non, émanant des établissements d'enseignement et de recherche français ou étrangers, des laboratoires publics ou privés.

Upsilon Production in Z Decays

The L3 Collaboration

Abstract

We have searched for evidence of Υ production in 3.5 million hadronic Z decays collected by the L3 detector at LEP in 1991-1995. No signals are observed for the decay chain $Z \rightarrow \Upsilon X$; $\Upsilon \rightarrow \ell^+ \ell^-$ ($\ell = e, \mu$), therefore upper limits at the 95% confidence level are set on the following Z branching fractions:

$$\text{Br}(Z \rightarrow \Upsilon(1S)X) < 5.5 \times 10^{-5};$$

$$\text{Br}(Z \rightarrow \Upsilon(2S)X) < 13.9 \times 10^{-5};$$

$$\text{Br}(Z \rightarrow \Upsilon(3S)X) < 9.4 \times 10^{-5}.$$

(Submitted to *Physics Letters B*)

Introduction

Recent theoretical predictions for Υ ¹⁾ production in hadronic Z decays [1] suggest that each LEP experiment should be able to observe a few Υ events using the decay modes $\Upsilon \rightarrow \ell^+ \ell^-$, where $\ell^+ \ell^-$ denotes either $e^+ e^-$ or $\mu^+ \mu^-$. Such an observation would support the novel colour-octet models which have been invoked to explain the anomalously high Υ production rates observed by the CDF Collaboration [2].

This paper describes the search for Υ production at LEP using the L3 detector, which is described elsewhere [3, 4]. The analysis uses a sample of approximately 3.5 million hadronic Z events acquired during 1991-1995 at $\sqrt{s} \approx M_Z$.

Simulation of Υ Production and Backgrounds

We have considered five distinct mechanisms for the production of (unpolarised) Υ 's in Z decays, as shown in Fig. 1. of Ref. 5. Table 1 shows the predicted branching ratios, $\text{Br}(Z \rightarrow \Upsilon X)$, for the colour-singlet (1–3) and colour-octet (4–5) processes. To study the sensitivity of the

Υ production mechanism	$\text{Br}(Z \rightarrow \Upsilon X) \times 10^5$
1. $Z \rightarrow \Upsilon b \bar{b}$ (b-quark fragmentation)	1.6 [6, 7]
2. $Z \rightarrow \Upsilon q \bar{q} g g$ (gluon fragmentation)	0.07 [8, 9]
3. $Z \rightarrow \Upsilon g g$ (gluon radiation)	0.05 [10–12]
4. $Z \rightarrow \Upsilon q \bar{q}$ (gluon fragmentation)	4.1 [1]
5. $Z \rightarrow \Upsilon g$ (gluon radiation)	0.1 [1]
Combined model	5.9

Table 1: Υ production mechanisms in Z decays and their predicted branching ratios.

L3 detector to events containing $\Upsilon \rightarrow \ell^+ \ell^-$ decays, we generate samples of 5000 $e^+ e^- \rightarrow \Upsilon X$ events, for each of these five production mechanisms using the OPAL implementation [5, 13] of the differential cross sections. The JETSET Monte Carlo program [14, 15] is used to simulate the subsequent parton showering, hadronisation, and particle decays. The Υ 's are required to decay via the chain $\Upsilon \rightarrow \ell^+ \ell^-$. Table 2 shows the masses and leptonic branching ratios of the $\Upsilon(1S)$, $\Upsilon(2S)$, and $\Upsilon(3S)$ which are assumed in this analysis [16]. A “combined model” sample is also used, which is the sum of the five distinct samples weighted according to the production rates predicted by the theory.

	Mass [GeV]	$\text{Br}(\Upsilon \rightarrow e^+ e^-)$ [%]	$\text{Br}(\Upsilon \rightarrow \mu^+ \mu^-)$ [%]
$\Upsilon(1S)$	9.460	2.52 ± 0.17	2.48 ± 0.07
$\Upsilon(2S)$	10.023	$\equiv \text{Br}(\Upsilon(2S) \rightarrow \mu^+ \mu^-)$	1.31 ± 0.21
$\Upsilon(3S)$	10.355	$\equiv \text{Br}(\Upsilon(3S) \rightarrow \mu^+ \mu^-)$	1.81 ± 0.17

Table 2: Properties of the $\Upsilon(1S)$, $\Upsilon(2S)$, and $\Upsilon(3S)$ assumed in this analysis.

¹⁾Throughout this paper, we use Υ to denote the three states $\Upsilon(1S)$, $\Upsilon(2S)$, and $\Upsilon(3S)$.

Υ production mechanism	$\varepsilon(Z \rightarrow \Upsilon X; \Upsilon \rightarrow \ell^+ \ell^-) [\%]$	
	e^+e^- channel	$\mu^+\mu^-$ channel
1. $Z \rightarrow \Upsilon b\bar{b}$	$37.4 \pm 0.6 \pm 5.0$	$21.2 \pm 0.5 \pm 2.6$
2. $Z \rightarrow \Upsilon q\bar{q}gg$	$25.5 \pm 0.6 \pm 3.4$	$14.3 \pm 0.5 \pm 1.7$
3. $Z \rightarrow \Upsilon gg$	$32.1 \pm 0.6 \pm 4.3$	$19.6 \pm 0.5 \pm 2.4$
4. $Z \rightarrow \Upsilon q\bar{q}$	$33.2 \pm 0.6 \pm 4.4$	$21.2 \pm 0.5 \pm 2.6$
5. $Z \rightarrow \Upsilon g$	$41.5 \pm 0.6 \pm 5.5$	$33.3 \pm 0.6 \pm 4.1$

Table 3: Efficiencies for the process $Z \rightarrow \Upsilon X; \Upsilon \rightarrow \ell^+ \ell^-$. The first error in each case is statistical and the second is systematic.

For the background studies a sample of approximately seven million hadronic events is generated using JETSET, not including the production of Υ 's. In addition, samples of 1000 four-fermion events are generated, using the FERMISV [17] Monte Carlo program, for each of the processes $e^+e^- \rightarrow \ell^+ \ell^- q\bar{q}$, where $\ell = e, \mu$ and $q = u, d, s, c, b$.

All the simulated events produced are passed through the GEANT-based L3 detector simulation program [18] and reconstructed using the same algorithms as for the data.

Event Selection

Hadronic events are selected by making use of their characteristic energy distributions and high multiplicity [19]. A total of $N_{\text{had}} = 3\,453\,780$ events pass the selection with an efficiency, determined from Monte Carlo, of $\varepsilon_{\text{had}} = 0.99 \pm 0.01$.

Candidate electrons with energies of more than 4 GeV are selected within $|\cos\theta| < 0.97$, where θ is the polar angle. An electron is characterised by an isolated energy cluster in the BGO electromagnetic calorimeter with a shower shape consistent with that of electromagnetic particles. To reject photons, the cluster is required to match with a charged track to within 5 mrad in the plane transverse to the beam direction. The transverse momentum of the track must be compatible with the cluster energy. Muon candidate tracks in the muon spectrometer, with momenta of more than 3 GeV, are required to be within $|\cos\theta| < 0.8$. The tracks must have hits in at least two of the three $r\phi$ layers and at least one of the two z layers. Backgrounds from punchthrough hadrons, decays in flight, and cosmic rays are suppressed by requiring the muon chamber track to point towards the primary vertex. To reject residual background from hadronic events, each candidate electron (muon) must be isolated by at least 10° (15°) from the closest jet, which may in some cases include another electron (muon) candidate. The event is required to contain either two electrons or two muons which satisfy these selection criteria. The lepton pairs are required to have opposite charges and to have an opening angle of less than 90° .

Figure 1 shows the expected dilepton invariant mass distributions for the “combined model” Monte Carlo sample after application of the selection procedure described above for a) $\Upsilon \rightarrow e^+e^-$, and b) $\Upsilon \rightarrow \mu^+\mu^-$. The shapes of the distributions for each individual Υ sample are similar. The average dilepton invariant mass resolutions are 100 MeV for electrons from $\Upsilon \rightarrow e^+e^-$ decays and 235 MeV for muons from $\Upsilon \rightarrow \mu^+\mu^-$ decays. Table 3 shows the efficiencies for each Υ production mechanism and decay mode, as determined from the Υ Monte Carlo samples. The efficiencies for the three Υ states differ, for a given model, by typically 0.5% for

the e^+e^- channel and 0.2% for the $\mu^+\mu^-$ channel. This variation is accounted for in the analysis. The systematic errors on the efficiencies are estimated by comparing the data and Monte Carlo distributions of the selection variables with various less stringent values for the cuts applied. Since no significant discrepancies are observed, the systematic errors are assigned according to the statistical accuracies of the comparisons. Uncertainties in the theoretical modelling which affect the efficiencies are treated explicitly, as described below.

Figure 1 shows the dilepton invariant mass spectra obtained from the data (solid line) for c) e^+e^- , and d) $\mu^+\mu^-$. No evidence is seen for Υ production in either of the decay modes considered. The dashed line represents the background contribution which is estimated from the Monte Carlo sample of hadronic Z and four-fermion events. For the e^+e^- channel the background is dominated by hadronic events in which a fake electron is paired with a genuine electron from a heavy-quark decay. For the $\mu^+\mu^-$ channel the background events are predominantly genuine muon pairs from the four-fermion process. The average number of background events expected in the mass window of 7–12 GeV is $10.3 \pm 2.0 \pm 1.1$ for the e^+e^- sample and $1.5 \pm 0.1 \pm 0.1$ events for the $\mu^+\mu^-$ sample, where the first error is due to the Monte Carlo statistics and the second is systematic. The number of events observed in the data are five and three for the e^+e^- and $\mu^+\mu^-$ samples respectively, which is consistent with the background.

Determination of Upper Limits on $\text{Br}(Z \rightarrow \Upsilon X)$

Given the absence of a signal, upper limits on the branching fractions $\text{Br}(Z \rightarrow \Upsilon X)$ are obtained from binned maximum-likelihood fits to the $\ell^+\ell^-$ invariant mass distributions. The likelihood function is given by:

$$\mathcal{L}(\text{Br}(Z \rightarrow \Upsilon X)) = \prod_{i=1}^{n_{\text{channels}}} \prod_{j=1}^{n_{\text{bins}}} \frac{\exp\left[-\left(\mu_{\text{bkg}}^{ij} + \mu_{\Upsilon}^{ij}\right)\right] \left(\mu_{\text{bkg}}^{ij} + \mu_{\Upsilon}^{ij}\right)^{N_{ij}}}{N_{ij}!} \quad (1)$$

where $i = 1, 2$ denotes the two Υ decay channels, $\Upsilon \rightarrow e^+e^-$ and $\Upsilon \rightarrow \mu^+\mu^-$; N_{ij} is the number of observed data events in mass bin j ; and μ_{Υ}^{ij} and μ_{bkg}^{ij} denote the expected numbers of events for signal and background, respectively. The expectation for the total number of $Z \rightarrow \Upsilon X; \Upsilon \rightarrow \ell_i^+ \ell_i^-$ events in the selected data sample is:

$$\mu_{\Upsilon}^i \equiv \sum_{j=1}^{n_{\text{bins}}} \mu_{\Upsilon}^{ij} = \left(\frac{N_{\text{had}}}{\varepsilon_{\text{had}} R_{\text{had}}} \right) \text{Br}(Z \rightarrow \Upsilon X) \text{Br}(\Upsilon \rightarrow \ell_i^+ \ell_i^-) \varepsilon(Z \rightarrow \Upsilon X; \Upsilon \rightarrow \ell_i^+ \ell_i^-), \quad (2)$$

where $R_{\text{had}} = 0.6990 \pm 0.0015$ [16] is the Z branching fraction to hadrons.

Separate limits are derived for each of the five production mechanisms considered and for each Υ state, assuming conservatively in each case that there is zero contribution from the other mechanisms and Υ states. Limits are also determined using the “combined model” sample. To facilitate comparison with other experiments, which do not resolve the $\Upsilon(1S)$, $\Upsilon(2S)$, and $\Upsilon(3S)$ states, we also derive limits for the production of an “average Υ ” which is an admixture of $\Upsilon(1S)$, $\Upsilon(2S)$, and $\Upsilon(3S)$. The range of relative fractions considered is discussed below. In deriving combined limits for different Υ states and theoretical models, the separate likelihoods are combined. The systematic errors, which are propagated numerically allowing for correlations, include contributions from the following sources:

Υ reconstruction efficiencies

The efficiencies are varied within the errors shown in Table 3. The statistical errors are uncorrelated for each model of a given sample. The systematic errors for a given decay mode are

completely correlated for all five models. The efficiency errors do not include uncertainties in the modelling which are treated explicitly, as described below.

Υ branching ratios

The uncertainties on the Υ leptonic branching ratios are shown in Table 2. The branching ratios $\text{Br}(\Upsilon(2\text{S}) \rightarrow e^+e^-)$ and $\text{Br}(\Upsilon(2\text{S}) \rightarrow \mu^+\mu^-)$ are completely correlated, as are $\text{Br}(\Upsilon(3\text{S}) \rightarrow e^+e^-)$ and $\text{Br}(\Upsilon(3\text{S}) \rightarrow \mu^+\mu^-)$.

Background

The uncertainties on the background for a given final state include statistical and systematic uncertainties for both the hadronic and the four-fermion components, as discussed above. The systematic uncertainties for the hadronic components are estimated by relaxing the selection cuts and comparing the data and Monte Carlo distributions of the selection variables. A common systematic error of 5% is assumed for the theoretical uncertainty on the four-fermion cross sections [17].

Number of Z events

The Z hadronic branching fraction, $R_{\text{had}} = 0.6990 \pm 0.0015$, and the hadronic event selection efficiency, $\varepsilon_{\text{had}} = 0.99 \pm 0.01$, are varied within their errors.

Invariant mass scale, resolution, fit range, and binning

The J peaks in the e^+e^- and $\mu^+\mu^-$ mass spectra are used to verify the di-lepton invariant mass scales and resolutions. The fitted J masses are 3083 ± 9 MeV and 3106 ± 13 MeV, for the e^+e^- and $\mu^+\mu^-$ final states, respectively, which are consistent with the current world average of $m_J = 3097$ MeV [16]. The e^+e^- and $\mu^+\mu^-$ invariant mass resolutions for data are 72 ± 10 MeV and 118 ± 13 MeV, respectively, which are in agreement with the Monte Carlo expectations of 66 ± 7 MeV and 107 ± 11 MeV. The Υ results are insensitive to changes of the mass scale or resolution, compatible with these measurements, and to the range and binning of the invariant mass distributions.

Υ polarisation

Since the Υ polarisation is unknown, we account for the changes in the efficiencies when going from the nominal flat distribution in $\cos\theta^*$ to a $1 + \cos^2\theta^*$ distribution, where θ^* is the lepton angle in the rest frame of the Υ . For the $1 + \cos^2\theta^*$ distribution the efficiencies are relatively lower with respect to the nominal values shown in Table 3 by between 6% and 13%, depending on the Υ production mechanism and decay mode.

Feed-down from higher-mass Υ and χ_b states

Feed-down decays from higher-mass Υ and χ_b states, with typical Q -values of less than 1 GeV, tend to soften the Υ momentum spectra. To estimate the impact on the reconstruction efficiency, we consider a scenario in which all Υ 's originate from higher states which decay with an average Q -value of 0.5 GeV. The resulting efficiencies are relatively lower by up to 4% with respect to the nominal values shown in Table 3.

Relative fractions of $\Upsilon(1\text{S})$, $\Upsilon(2\text{S})$, and $\Upsilon(3\text{S})$ states

The relative fractions of $\Upsilon(1\text{S})$, $\Upsilon(2\text{S})$, and $\Upsilon(3\text{S})$ which are assumed for the definition of the “average Υ ” depend on the amount of feed-down from the $\Upsilon(2\text{S})$, $\Upsilon(3\text{S})$, and χ_b states. The effect of feed-down is to enhance the contribution of the lower-mass Υ 's compared to the higher-mass Υ 's. For example, for a $\frac{1}{3} : \frac{1}{3} : \frac{1}{3}$ initial admixture of $\Upsilon(1\text{S})$, $\Upsilon(2\text{S})$, and $\Upsilon(3\text{S})$, the relative proportions after allowing only for measured Υ decays [16] are approximately 0.46:0.27:0.27.

Since the decay modes and relative production rates of the various Υ and χ_b states are poorly known, we consider the range of relative weights from $\frac{1}{3} : \frac{1}{3} : \frac{1}{3}$ to 1:0:0.

Table 4 summarises the upper limits obtained at the 95% confidence level (C.L.). The upper limit of $\text{Br}(Z \rightarrow \Upsilon X) < 7.6 \times 10^{-5}$ is consistent with the theoretical prediction of $\text{Br}(Z \rightarrow \Upsilon X) = 5.9 \times 10^{-5}$, shown in Table 1, and previous less stringent upper limits from LEP [20,21]. Consistency with the OPAL measurement of $\text{Br}(Z \rightarrow \Upsilon X) = (10 \pm 4 \pm 1) \times 10^{-5}$ [5] is marginal.

Υ production mechanism	Upper limit on $\text{Br}(Z \rightarrow \Upsilon X) \times 10^5$ at the 95% C.L.			
	$\Upsilon(1S)$	$\Upsilon(2S)$	$\Upsilon(3S)$	Average Υ
1. $Z \rightarrow \Upsilon b\bar{b}$	5.4	13.5	9.0	7.4
2. $Z \rightarrow \Upsilon q\bar{q}gg$	7.8	16.3	13.0	10.5
3. $Z \rightarrow \Upsilon gg$	6.0	14.1	9.9	8.0
4. $Z \rightarrow \Upsilon q\bar{q}$	5.5	14.0	9.5	7.6
5. $Z \rightarrow \Upsilon g$	3.9	10.3	6.9	5.4
Combined model	5.5	13.9	9.4	7.6

Table 4: Upper limits on the branching ratios for the process $Z \rightarrow \Upsilon X$, at the 95% confidence level. The “Average Υ ” is an admixture of $\Upsilon(1S)$, $\Upsilon(2S)$, and $\Upsilon(3S)$, as described in the text. The “combined model” corresponds to the sum of the five Υ production mechanisms, weighted according to their predicted rates and reconstruction efficiencies.

Acknowledgements

We wish to express our gratitude to the CERN accelerator divisions for the excellent performance of the LEP machine. We acknowledge with appreciation the effort of all engineers, technicians and support staff who have participated in the construction and maintenance of this experiment.

References

- [1] P. Cho, Phys. Lett. **B368** (1996) 171.
- [2] CDF Collab., F. Abe *et al.*, Phys. Rev. Lett. **75** (1995) 4358.
- [3] L3 Collab., B. Adeva *et al.*, Nucl. Instr. and Meth. **A289** (1990) 35.
- [4] L3 Collab., O. Adriani *et al.*, Physics Reports **236** (1993) 1.
- [5] OPAL Collab., G. Alexander *et al.*, Phys. Lett. **B 370** (1996) 185.
- [6] E. Braaten, K. Cheung and T.C. Yuan, Phys. Rev. **D48** (1993) 4230.
- [7] V. Barger, K. Cheung and W.Y. Keung, Phys. Rev. **D41** (1990) 1541.
- [8] E. Braaten and T.C. Yuan, Phys. Rev. Lett. **71** (1993) 1673.
- [9] K. Hagiwara *et al.*, Phys. Lett. **B267** (1991) 527, Erratum: Phys. Lett. **B316** (1993) 631.
- [10] K.J. Abraham, Zeit. für Phys. **C44** (1989) 467.
- [11] J.H. Kühn and H. Schneider, Zeit. für Phys. **C11** (1981) 263.
- [12] W.Y. Keung, Phys. Rev. **D23** (1981) 2072.
- [13] We are grateful to F. Odorici and E. Ros for making available to us the OPAL implementation of the differential cross sections for Υ production in Z decays.
- [14] T. Sjöstrand and M. Bengtsson, Comput. Phys. Commun. **43** (1987) 367.
- [15] T. Sjöstrand and M. Bengtsson, CERN Preprint CERN-TH **6488/92** (1992).
- [16] Particle Data Group, R. M. Barnett *et al.*, Phys. Rev. **D54** (1996) 1.
- [17] J. Hilgart, R. Kleiss and F. Le Diberder, Comput. Phys. Commun. **75** (1993) 191.
- [18] The L3 detector simulation program is based on GEANT Version 3.15 (see: R. Brun *et al.*, “GEANT 3”, CERN DD/EE/84-1 revised, (1987)). GHEISHA is used to simulate hadronic interactions (see: H. Fesefeldt, RWTH Aachen Report PITHA 85/02 (1985)). This program allows for the effects of energy loss, multiple scattering, decays and interactions in the detector material, as well as for time-dependent detector effects.
- [19] L3 Collab., O. Adriani *et al.*, Phys. Lett. **B307** (1993) 237.
- [20] ALEPH Collab., “Inclusive Υ production in hadronic Z decays”, In Proceedings of ICHEP96, PA05-066, Warsaw, 25-31 July (1996).
- [21] DELPHI Collab., P. Abreu *et al.*, Zeit. für Phys. **C 69** (1996) 575.

The L3 Collaboration:

M. Acciarri;²⁸ O. Adriani;¹⁷ M. Aguilar-Benitez;²⁷ S. Ahlen;¹¹ J. Alcaraz;²⁷ G. Alemani;²³ J. Allaby;¹⁸ A. Aloisio;³⁰ G. Alverson;¹² M. G. Alvigi;³⁰ G. Ambrosi;²⁰ H. Anderhub;⁵⁰ V. P. Andreev;³⁹ T. Angelescu;¹³ F. Anselmo;⁹ A. Arefiev;²⁹ T. Azemoon;³ T. Aziz;¹⁰ P. Bagnaia;³⁸ L. Baksay;⁴⁵ R. C. Ball;³ S. Banerjee;¹⁰ Sw. Banerjee;¹⁰ K. Banicz;⁴⁷ A. Barczyk;^{50,48} R. Barillere;¹⁸ L. Barone;³⁸ P. Bartalini;³⁵ A. Baschirotto;²⁸ M. Basile;⁹ R. Battiston;³⁵ A. Bay;²³ F. Becattini;¹⁷ U. Becker;¹⁶ F. Behner;⁵⁰ J. Berdugo;²⁷ P. Berges;¹⁶ B. Bertucci;³⁵ B. L. Betev;⁵⁰ S. Bhattacharya;¹⁰ M. Biasini;¹⁸ A. Biland;⁵⁰ G. M. Bilei;³⁵ J. J. Blaising;⁴ S. C. Blyth;³⁶ G. J. Bobbink;² R. Bock;¹ A. Böhm;¹ L. Boldizsar;¹⁴ B. Borgia;³⁸ A. Boucham;⁴ D. Bourilkov;⁵⁰ M. Bourquin;²⁰ D. Boutigny;⁴ S. Braccini;²⁰ J. G. Branson;⁴¹ V. Brigljevic;⁵⁰ I. C. Brock;³⁶ A. Buffini;¹⁷ A. Buijs;⁴⁶ J. D. Burger;¹⁶ W. J. Burger;²⁰ J. Busenitz;⁴⁵ X. D. Cai;¹⁶ M. Campanelli;⁵⁰ M. Capell;¹⁶ G. Cara Romeo;⁹ G. Carloni;³⁰ A. M. Cartacci;¹⁷ J. Casaus;²⁷ G. Castellini;¹⁷ F. Cavallari;³⁸ N. Cavallo;³⁰ C. Cecchi;²⁰ M. Cerrada;²⁷ F. Cesaroni;²⁴ M. Chamizo;²⁷ Y. H. Chang;⁵² U. K. Chaturvedi;¹⁹ S. V. Chekanov;³² M. Chemarin;²⁶ A. Chen;⁵² G. Chen;⁷ G. M. Chen;⁷ H. F. Chen;²¹ H. S. Chen;⁷ M. Chen;¹⁶ G. Chiefari;³⁰ C. Y. Chien;⁵ L. Cifarelli;⁴⁰ F. Cindolo;⁹ C. Civinini;¹⁷ I. Clare;¹⁶ R. Clare;¹⁶ H. O. Cohn;³ G. Coignet;⁴ A. P. Colijn;² N. Colino;²⁷ V. Commichau;¹ S. Costantini;⁸ F. Cotorobai;¹³ B. de la Cruz;²⁷ A. Csilling;¹⁴ T. S. Dai;¹⁶ R. D' Alessandro;¹⁷ R. de Asmundis;³⁰ A. Degré;⁴ K. Deiters;⁴⁸ P. Denes;³⁷ F. DeNotaristefani;³⁸ D. DiBitonto;⁴⁵ M. Diemoz;³⁸ D. van Dierendonck;² F. Di Lodovico;⁵⁰ C. Dionisi;³⁸ M. Dittmar;⁵⁰ A. Dominguez;⁴¹ A. Doria;³⁰ I. Dorne;⁴ M. T. Dova;^{19,4} E. Drago;³⁰ D. Duchesneau;⁴ P. Duinker;² I. Duran;⁴² S. Dutta;¹⁰ S. Easo;³⁵ Yu. Efremenko;³³ H. El Mamouni;²⁶ A. Engler;³⁶ F. J. Eppinger;¹⁶ F. C. Erne;² J. P. Ernenwein;²⁶ P. Extermann;²⁰ M. Fabre;⁴⁸ R. Faccini;³⁸ S. Falciano;³⁸ A. Favara;¹⁷ J. Fay;²⁶ O. Fedin;³⁹ M. Felcini;⁵⁰ B. Fenyi;⁴⁵ T. Ferguson;³⁶ F. Ferroni;³⁸ H. Fesefeldt;¹ E. Fiandrini;³⁵ J. H. Field;²⁰ F. Filthaut;³⁶ P. H. Fisher;¹⁶ I. Fisk;⁴¹ G. Forconi;¹⁶ L. Fredj;²⁰ K. Freudenreich;⁵⁰ C. Furetta;²⁸ Yu. Galaktionov;^{29,16} S. N. Ganguli;¹⁰ P. Garcia-Abia;⁴⁹ S. S. Gau;¹² S. Gentile;³⁸ J. Gerald;⁵ N. Gheordanescu;¹³ S. Giagu;³⁸ S. Goldfarb;²³ J. Goldstein;¹¹ Z. F. Gong;²¹ A. Gougas;⁵ G. Gratta;³⁴ M. W. Gruenewald;⁸ V. K. Gupta;³⁷ A. Gurtu;¹⁰ L. J. Gutay;⁴⁷ B. Hartmann;¹ A. Hasan;³¹ D. Hatzifotiadou;³ T. Hebbeker;⁸ A. Hervé;¹⁸ W. C. van Hoek;³² H. Hofer;⁵⁰ S. J. Hong;⁴⁴ H. Hoorani;³⁶ S. R. Hou;⁵² G. Hu;⁵ V. Innocente;¹⁸ H. Janssen;⁴ K. Jenkes;¹ B. N. Jin;⁷ L. W. Jones;³ P. de Jong;¹⁸ I. Josa-Mutuberria;²⁷ A. Kasser;²³ R. A. Khan;¹⁹ D. Kamrad;⁴⁹ Yu. Kamyshev;³³ J. S. Kapustinsky;²⁵ Y. Karyotakis;⁴ M. Kaur;^{19,4} M. N. Kienzle-Focacci;²⁰ D. Kim;³⁸ D. H. Kim;⁴⁴ J. K. Kim;⁴⁴ S. C. Kim;⁴⁴ Y. G. Kim;⁴⁴ W. W. Kinnison;²⁵ A. Kirkby;³⁴ D. Kirkby;³⁴ J. Kirkby;¹⁸ D. Kiss;¹⁴ W. Kittel;³² A. Klimentov;^{16,29} A. C. König;³² A. Kopp;⁴⁹ I. Korolko;²⁹ V. Koutsenko;^{16,29} R. W. Kraemer;³⁶ W. Krenz;¹ A. Kunin;^{16,29} P. Ladron de Guevara;²⁷ G. Landi;¹⁷ C. Lapoint;¹⁶ K. Lassila-Perini;⁵⁰ P. Laurikainen;²² M. Lebeau;¹⁸ A. Lebedev;¹⁶ P. Lebrun;²⁶ P. Lecomte;⁵⁰ P. Lecoq;¹⁸ P. Le Coultre;³⁸ C. Leggett;³ J. M. Le Goff;¹⁸ R. Leiste;⁴⁹ E. Leonardi;³⁸ P. Levchenko;³⁹ C. Li;²¹ C. H. Lin;⁵² W. T. Lin;⁵² F. L. Linde;^{2,18} L. Lista;³⁰ Z. A. Liu;⁷ W. Lohmann;⁴⁹ E. Longo;³⁸ W. Lu;³⁴ Y. S. Lu;⁷ K. Lübelmeyer;¹ C. Luci;³⁸ D. Luckey;¹⁶ L. Luminari;³⁸ W. Lustermann;⁴⁸ W. G. Ma;²¹ M. Maity;¹⁰ G. Majumder;¹⁰ L. Malgeri;³⁸ A. Malinin;²⁹ C. Mañá;²⁷ D. Mangeol;³² S. Mangla;¹⁰ P. Marchesini;⁵⁰ A. Marin;¹¹ J. P. Martin;²⁶ F. Marzano;³⁸ G. G. G. Massaro;² D. McNally;¹⁸ S. Mele;³⁰ L. Merola;³⁰ M. Meschini;¹⁷ W. J. Metzger;³² M. von der Mey;¹ Y. Mi;²³ A. Mihul;¹³ A. J. W. van Mil;³² G. Mirabelli;³⁸ J. Mnich;¹⁸ P. Molnar;⁸ B. Monteleoni;¹⁷ R. Moore;³ S. Morganti;³⁸ T. Moulik;¹⁰ R. Mount;³⁴ S. Müller;¹ F. Muheim;²⁰ A. J. M. Muijs;² S. Nahn;¹⁶ M. Napolitano;³⁰ F. Nessi-Tedaldi;⁵⁰ H. Newman;³⁴ T. Niessen;¹ A. Nippe;¹ A. Nisati;³⁸ H. Nowak;⁴⁹ Y. D. Oh;⁴⁴ H. Opitz;¹ G. Organtini;³⁸ R. Ostonen;²² C. Palomares;²⁷ D. Pandoulas;¹ S. Paoletti;³⁸ P. Paolucci;³⁰ H. K. Park;³⁶ I. H. Park;⁴⁴ G. Pascale;³⁸ G. Passaleva;¹⁷ S. Patricelli;³⁰ T. Paul;¹² M. Pauluzzi;³⁵ C. Paus;¹ F. Pauss;⁵⁰ D. Peach;¹⁸ Y. J. Pei;¹ S. Pensotti;²⁸ D. Perret-Gallix;⁴ B. Petersen;³² S. Petrak;⁸ A. Pevsner;⁵ D. Piccolo;³⁰ M. Pieri;¹⁷ J. C. Pinto;³⁶ P. A. Piroué;³⁷ E. Pistolesi;²⁸ V. Plyaskin;²⁹ M. Pohl;⁵⁰ V. Pojidaev;^{29,17} H. Postema;¹⁶ N. Produit;²⁰ D. Prokofiev;³⁹ G. Rahal-Callot;⁵⁰ N. Raja;¹⁰ P. G. Rancoita;²⁸ M. Rattaggi;²⁸ G. Raven;⁴¹ P. Razis;³¹ K. Read;³³ D. Ren;⁵⁰ M. Rescigno;³⁸ S. Reucroft;¹² T. van Rhee;⁴⁶ S. Riemann;⁴⁹ K. Riles;³ O. Rind;³ A. Robohm;⁵⁰ J. Rodin;¹⁶ B. P. Roe;³ L. Romero;²⁷ S. Rosier-Lees;⁴ Ph. Rosselet;²³ W. van Rossum;⁴⁶ S. Roth;¹ J. A. Rubio;¹⁸ D. Ruschmeier;⁸ H. Rykaczewski;⁵⁰ J. Salicio;¹⁸ E. Sanchez;²⁷ M. P. Sanders;³² M. E. Sarakinos;²² S. Sarkar;¹⁰ M. Sassowsky;¹ G. Sauvage;⁴ C. Schäfer;¹ V. Schegelsky;³⁹ S. Schmidt-Kaerst;¹ D. Schmitz;¹ P. Schmitz;¹ M. Schneegans;⁴ N. Scholz;⁵⁰ H. Schopper;⁵¹ D. J. Schotanus;³² J. Schwenke;¹ G. Schwering;¹ C. Sciacca;³⁰ D. Sciarrino;²⁰ L. Servoli;³⁵ S. Shevchenko;³⁴ N. Shivarov;⁴³ V. Shoutko;²⁹ J. Shukla;²⁵ E. Shumilov;²⁹ A. Shvorob;³⁴ T. Siedenburgh;¹ D. Son;⁴⁴ A. Sopczak;⁴⁹ V. Soulimov;³⁰ B. Smith;¹⁶ P. Spillantini;¹⁷ M. Steuer;¹⁶ D. P. Stickland;³⁷ H. Stone;³⁷ B. Stoyanov;⁴³ A. Straessner;¹ K. Strauch;¹⁵ K. Sudhakar;¹⁰ G. Sultanov;¹⁹ L. Z. Sun;²¹ G. F. Susinno;²⁰ H. Suter;⁵⁰ J. D. Swain;¹⁹ X. W. Tang;⁷ L. Tauscher;⁶ L. Taylor;¹² Samuel C. C. Ting;¹⁶ S. M. Ting;¹⁶ M. Tonutti;¹ S. C. Tonwar;¹⁰ J. Tóth;¹⁴ C. Tully;³⁷ H. Tuchscherer;⁴⁵ K. L. Tung;⁷ Y. Uchida;¹⁶ J. Ulbricht;⁵⁰ U. Uwer;¹⁸ E. Valente;³⁸ R. T. Van de Walle;³² G. Vesztegombi;¹⁴ I. Vetlitsky;²⁹ G. Viertel;⁵⁰ M. Vivargent;⁴ R. Völkert;⁴⁹ H. Vogel;³⁶ H. Vogt;⁴⁹ I. Vorobiev;²⁹ A. A. Vorobyov;³⁹ A. Vorvolakos;³¹ M. Wadhwa;⁶ W. Wallraff;¹ J. C. Wang;¹⁶ X. L. Wang;²¹ Z. M. Wang;²¹ A. Weber;¹ F. Wittgenstein;¹⁸ S. X. Wu;¹⁹ S. Wynhoff;¹ J. Xu;¹ Z. Z. Xu;²¹ B. Z. Yang;²¹ C. G. Yang;⁷ X. Y. Yao;⁷ J. B. Ye;²¹ S. C. Yeh;⁵² J. M. You;³⁶ An. Zalite;³⁹ Yu. Zalite;³⁹ P. Zemp;⁵⁰ Y. Zeng;¹ Z. Zhang;⁷ Z. P. Zhang;²¹ B. Zhou;¹¹ Y. Zhou;³ G. Y. Zhu;⁷ R. Y. Zhu;³⁴ A. Zichichi;^{9,18,19} F. Ziegler;⁴⁹

- 1 I. Physikalisches Institut, RWTH, D-52056 Aachen, FRG[§]
 - III. Physikalisches Institut, RWTH, D-52056 Aachen, FRG[§]
 - 2 National Institute for High Energy Physics, NIKHEF, and University of Amsterdam, NL-1009 DB Amsterdam, The Netherlands
 - 3 University of Michigan, Ann Arbor, MI 48109, USA
 - 4 Laboratoire d'Annecy-le-Vieux de Physique des Particules, LAPP, IN2P3-CNRS, BP 110, F-74941 Annecy-le-Vieux CEDEX, France
 - 5 Johns Hopkins University, Baltimore, MD 21218, USA
 - 6 Institute of Physics, University of Basel, CH-4056 Basel, Switzerland
 - 7 Institute of High Energy Physics, IHEP, 100039 Beijing, China[△]
 - 8 Humboldt University, D-10099 Berlin, FRG[§]
 - 9 University of Bologna and INFN-Sezione di Bologna, I-40126 Bologna, Italy
 - 10 Tata Institute of Fundamental Research, Bombay 400 005, India
 - 11 Boston University, Boston, MA 02215, USA
 - 12 Northeastern University, Boston, MA 02115, USA
 - 13 Institute of Atomic Physics and University of Bucharest, R-76900 Bucharest, Romania
 - 14 Central Research Institute for Physics of the Hungarian Academy of Sciences, H-1525 Budapest 114, Hungary[‡]
 - 15 Harvard University, Cambridge, MA 02139, USA
 - 16 Massachusetts Institute of Technology, Cambridge, MA 02139, USA
 - 17 INFN Sezione di Firenze and University of Florence, I-50125 Florence, Italy
 - 18 European Laboratory for Particle Physics, CERN, CH-1211 Geneva 23, Switzerland
 - 19 World Laboratory, FBLJA Project, CH-1211 Geneva 23, Switzerland
 - 20 University of Geneva, CH-1211 Geneva 4, Switzerland
 - 21 Chinese University of Science and Technology, USTC, Hefei, Anhui 230 029, China[△]
 - 22 SEFT, Research Institute for High Energy Physics, P.O. Box 9, SF-00014 Helsinki, Finland
 - 23 University of Lausanne, CH-1015 Lausanne, Switzerland
 - 24 INFN-Sezione di Lecce and Università Degli Studi di Lecce, I-73100 Lecce, Italy
 - 25 Los Alamos National Laboratory, Los Alamos, NM 87544, USA
 - 26 Institut de Physique Nucléaire de Lyon, IN2P3-CNRS, Université Claude Bernard, F-69622 Villeurbanne, France
 - 27 Centro de Investigaciones Energeticas, Medioambientales y Tecnológicas, CIEMAT, E-28040 Madrid, Spain[‡]
 - 28 INFN-Sezione di Milano, I-20133 Milan, Italy
 - 29 Institute of Theoretical and Experimental Physics, ITEP, Moscow, Russia
 - 30 INFN-Sezione di Napoli and University of Naples, I-80125 Naples, Italy
 - 31 Department of Natural Sciences, University of Cyprus, Nicosia, Cyprus
 - 32 University of Nijmegen and NIKHEF, NL-6525 ED Nijmegen, The Netherlands
 - 33 Oak Ridge National Laboratory, Oak Ridge, TN 37831, USA
 - 34 California Institute of Technology, Pasadena, CA 91125, USA
 - 35 INFN-Sezione di Perugia and Università Degli Studi di Perugia, I-06100 Perugia, Italy
 - 36 Carnegie Mellon University, Pittsburgh, PA 15213, USA
 - 37 Princeton University, Princeton, NJ 08544, USA
 - 38 INFN-Sezione di Roma and University of Rome, "La Sapienza", I-00185 Rome, Italy
 - 39 Nuclear Physics Institute, St. Petersburg, Russia
 - 40 University and INFN, Salerno, I-84100 Salerno, Italy
 - 41 University of California, San Diego, CA 92093, USA
 - 42 Dept. de Física de Partículas Elementales, Univ. de Santiago, E-15706 Santiago de Compostela, Spain
 - 43 Bulgarian Academy of Sciences, Central Lab. of Mechatronics and Instrumentation, BU-1113 Sofia, Bulgaria
 - 44 Center for High Energy Physics, Korea Adv. Inst. of Sciences and Technology, 305-701 Taejeon, Republic of Korea
 - 45 University of Alabama, Tuscaloosa, AL 35486, USA
 - 46 Utrecht University and NIKHEF, NL-3584 CB Utrecht, The Netherlands
 - 47 Purdue University, West Lafayette, IN 47907, USA
 - 48 Paul Scherrer Institut, PSI, CH-5232 Villigen, Switzerland
 - 49 DESY-Institut für Hochenergiephysik, D-15738 Zeuthen, FRG
 - 50 Eidgenössische Technische Hochschule, ETH Zürich, CH-8093 Zürich, Switzerland
 - 51 University of Hamburg, D-22761 Hamburg, FRG
 - 52 High Energy Physics Group, Taiwan, China
- § Supported by the German Bundesministerium für Bildung, Wissenschaft, Forschung und Technologie
- ‡ Supported by the Hungarian OTKA fund under contract numbers T14459 and T24011.
- ‡ Supported also by the Comisión Interministerial de Ciencia y Tecnología
- ‡ Also supported by CONICET and Universidad Nacional de La Plata, CC 67, 1900 La Plata, Argentina
- △ Also supported by Panjab University, Chandigarh-160014, India
- △ Supported by the National Natural Science Foundation of China.

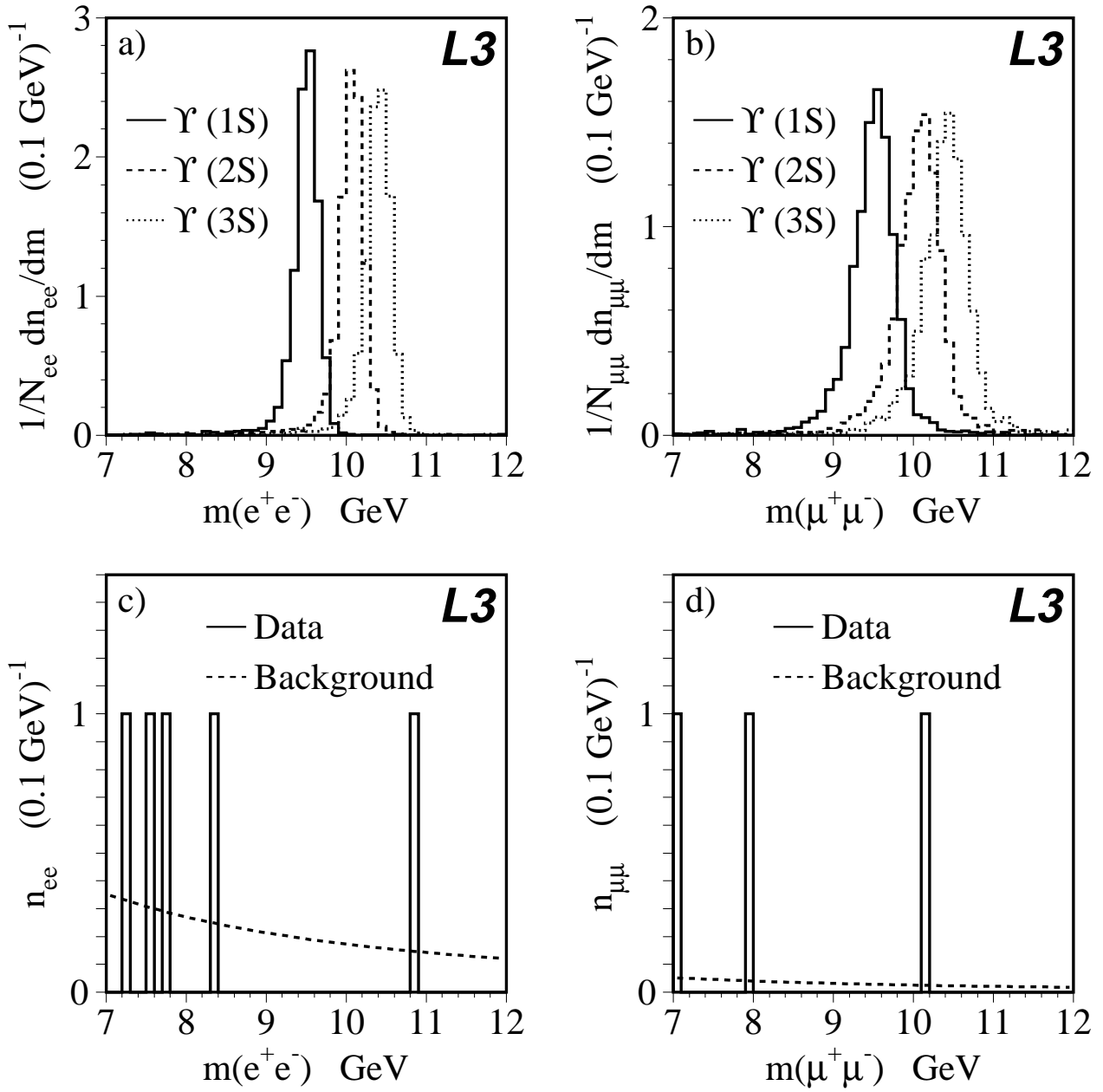


Figure 1: Predictions for the dilepton invariant mass distributions for a) $\Upsilon \rightarrow e^+e^-$, and b) $\Upsilon \rightarrow \mu^+\mu^-$ decays. Invariant mass spectra obtained from the data (solid line) for c) e^+e^- , and d) $\mu^+\mu^-$; the dashed lines show the background predicted by the Monte Carlo. The number of selected dilepton candidates in a given bin is denoted by $n_{\ell\ell}$ ($\ell = e, \mu$) while $N_{\ell\ell}$ denotes the total number in the sample.